
Molecular Crystals and Liquid Crystals
Publication details, including instructions for authors and subscription information:
http://www.tandfonline.com/loi/gmcl16

# Correlations of Anion Size and Symmetry with the Structure and Electronic Properties of β-(BEDTTTF)$_2$X Conducting Salts with Trihalide Anions X = $1_3$-, $1_2Br$-, $1Br_2$-

Thomas J. Emge [a], Peter C. W. Leung [a], Mark A. Beno [a], Hau H. Wang [a], M. A. Firestone [a], Kevin S. Webb [a], K. Douglas Carlson [a], Jack M. Williams [a], E. L. Venturini [b], L. J. Azevedo [b] & J. E. Schirber [b]

[a] Chemistry and Materials Science and Technology Divisions, Argonne National Laboratory, Argonne, IL, 60439

[b] Sandia National Laboratory, Albuquerque, New Mexico, 87185

Version of record first published: 20 Apr 2011.

*Mol. Cryst. Liq. Cryst.*, 1986, Vol. 132, pp. 363–383
0026-8941/86/1324–0363/$25.00/0

Printed in the United States of America



# Correlations of Anion Size and Symmetry with the Structure and Electronic Properties of β-(BEDT-TTF)$_2$X Conducting Salts with Trihalide Anions X = $I_3^-$, $I_2Br^-$, $IBr_2^-$

THOMAS J. EMGE, PETER C. W. LEUNG, MARK A. BENO, HAU H. WANG, M. A. FIRESTONE,[44a] KEVIN S. WEBB,[44b] K. DOUGLAS CARLSON and JACK M. WILLIAMS†

*Chemistry and Materials Science and Technology Divisions, Argonne National Laboratory, Argonne, IL 60439*

and

E. L. VENTURINI, L. J. AZEVEDO and J. E. SCHIRBER

*Sandia National Laboratory, Albuquerque, New Mexico 87185*

(*Received June 21, 1985*)

In the isostructural series of β-(BEDT-TTF)$_2$X organic metals, abbreviated β-(ET)$_2$X, where X is a trihalide anion, $I_3^-$, $I_2Br^-$ or $IBr_2^-$, and where ET is bis-(ethylenedithio)tetrathiafulvalene ($C_{10}S_8H_8$), the salt containing the disordered *asymmetric* $I_2Br^-$ anion has atypical structural and electronic properties compared to those containing the *symmetrical* and ordered $I_3^-$ and $IBr_2^-$ anions. Ambient pressure superconductivity has been detected in the salts containing the *symmetrical* anions, viz. β-(ET)$_2I_3$ ($T_c$ = 1.4 K) and β-(ET)$_2IBr_2$ ($T_c$ = 2.8 K), but not in that which contains the *asymmetric* anion, β-(ET)$_2I_2Br$, even though the $I_2Br^-$ anion is of length intermediate between $I_3^-$ and $IBr_2^-$. Low field esr measurements reveal that the metallic state in β-(ET)$_2I_2Br$ persists to 1.07 K and also up to 5 kbar pressure. The *absence* of superconductivity, even under modest pressure, appears to be the result of the disordering of the $I_2Br^-$

†Author to whom correspondence should be addressed.

anion. For these three isostructural β-$(ET)_2X$ salts, the crystal packing of the ET molecules consists of a tightly packed two-dimensional network, with *inter*stack S···S contacts that are often less than the van der Waals radii sum of 3.60 Å, and H···X interactions (X = I or Br) that serve to connect the cation networks with the anions that reside between the networks. Correlations between anion size and the intermolecular S···S and H···X distances are discussed. Unit cell lattice parameters (298/120 K) for these three isostructural salts (space group $P\bar{1}$, Z = 1) are for β-$(ET)_2I_3$: $a$ = 6.615(1)/6.561(1) Å, $b$ = 9.100(1)/9.013(2) Å, $c$ = 15.286(2)/15.173(2) Å, α = 94.38(1)/95.07(1)°, β = 95.59(1)/95.93(1)°, γ = 109.78(1)/110.28(1)°, V = 855.9(2)/829.2(3) Å$^3$; for β-$(ET)_2I_2Br$: $a$ = 6.612(1)/6.613(1) Å, $b$ = 9.024(2)/8.873(2) Å, $c$ = 15.192(2)/15.100(2) Å, α = 94.16(1)/95.64(1)°, β = 95.23(1)/95.15(1)°, γ = 110.12(1)/109.79(1)°, V = 842.3(3)/822.4(2) Å$^3$; and for β-$(ET)_2IBr_2$: $a$ = 6.593(1)/6.589(1) Å, $b$ = 8.975(2)/8.820(2) Å, $c$ = 15.093(5)/14.988(5) Å, α = 93.79(2)/95.30(2)°, β = 94.96(2)/94.87(2)°, γ = 110.54(2)/110.28(2)°, V = 828.7(5)/807.1(5) Å$^3$.

*Keywords: organic metals, ET-based, anion size, structures*

## INTRODUCTION

The first discovery of superconductivity in an organic molecular system was in several isostructural $(TMTSF)_2X$ salts (X = $ClO_4^-$, $ReO_4^-$, $PF_6^-$, $AsF_6^-$, $TaF_6^-$ and $SbF_6^-$), where TMTSF is tetramethyltetraselenafulvalene, ($C_{10}H_{12}Se_4$).[1-7] In order to achieve superconductivity, all of the $(TMTSF)_2X$ salts *except* $(TMTSF)_2ClO_4$ ($T_c$ = ~1.2 K) require high pressure (~10 kbar), which in several salts including X = $ReO_4^-$, $PF_6^-$ and $AsF_6^-$, suppresses a metal-insulator [MI] transition.[8-10] Among the driving forces for the MI transitions in $(TMTSF)_2X$ salts, anion-ordering (AO)[11] phenomena near the MI transition temperature ($T_{MI}$) have been studied.[12,13] For the X = $ClO_4^-$, $ReO_4^-$, $BF_4^-$, and $NO_3^-$ (acentric anions) salts, dramatic structural changes and crystallographic transitions result from *anion ordering* that involves a doubling of "high-temperature" lattice constants after cooling through $T_{MI}$.[12,14-16] The sole Se-based ambient pressure superconductor, $(TMTSF)_2ClO_4$ becomes superconducting only when *slowly* cooled (i.e., <4K/min), which results in an *ordered* anion state. The absence of superconductivity in the fast-cooled (quenched state) samples of $(TMTSF)_2ClO_4$ has been attributed to the "frozen" *disordered* anion state.[17,18]

The interactions between the TMTSF radical cations and the anions can be characterized in terms of Se···X and H···X contacts, which play a major role in anion disorder-order transitions.[14-16] From x-ray diffraction results,[19] the derived Se···Se, Se···X and H···X distances (with respect to the associated van der Waals radii[20]) form the basis of structure-property correlations[19,21] for the $(TMTSF)_2X$ salts. These correlations are possible despite the diversity of anion shapes

(tetrahedral, octahedral, planar etc.) and sizes, because of the common cation-cation network in their isostructural salts. In like fashion, the examination of *isostructural* $\beta$-$(ET)_2X$ salts leads to significant structure-property correlations (vide infra).

The search for new organic superconductors has been immensely successful with the synthesis of $(BEDT\text{-}TTF)_2X$ salts,[22-25] where BEDT-TTF (**1**), abbreviated herein as "ET," is bis-(ethylenedithio)tetrathiafulvalene, ($C_{10}H_8S_8$). Ambient

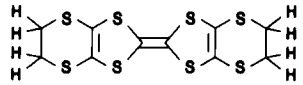

**BEDT-TTF (ET)**

pressure superconductivity (SC) has been discovered in $\beta$-$(ET)_2I_3$ ($T_c \sim 1.4$ K)[26,27] and $\beta$-$(ET)_2IBr_2$ ($T_c \sim 2.8$ K).[28,29] The requirement of pressure to attain the SC state, as observed for several $(TMTSF)_2X$ salts, is also the case for the first $(ET)_2X$ superconductor, $(ET)_2ReO_4$ ($P = 4$ kbar, $T_c = 2$ K), which otherwise undergoes an MI transition at 80 K at ambient pressure.[25] In contrast to the $(TMTSF)_2X$ salts, several phases of ET:X crystals may simultaneously grow during electrocrystallization. The crystal and electrical properties of the $\beta$-phases of $(ET)_2X$ ($X = I_3^-$ or $IBr_2^-$)[29-31] are quite different from that of $\alpha$-$(ET)_2I_3$.[32] Although both the $\alpha$ and $\beta$ phases of $(ET)_2I_3$ are metallic at room temperature, $\alpha$-$(ET)_2I_3$ undergoes an MI transition[32] at 135 K, while the $\beta$-phase remains metallic down to $T_c$.[26,27,31] The many phases of ET:X salts have different electronic ground states, ranging from insulating to metallic.[26,33] The $\alpha$ and $\beta$ phases can be separated by use of their differing ESR linewidths[34] (vide infra).

The structural motifs of several $(ET)_2X$ salts (i.e., $X = I_3^-$, $IBr_2^-$, $ReO_4^-$, $ClO_4^-$, $PF_6^-$) bear some similarity to that of the $(TMTSF)_2X$ salts. Alternating between the 2-D networks of interacting radical cations, there are anions ($X^-$) that engage in cation-anion interactions via H···X contacts. A structural study of the isostructural series of $\beta$-$(ET)_2X$ salts, $X = I_3^-$, $I_2Br^-$ and $IBr_2^-$, provides an opportunity to investigate the small, but systematic, variations of the 2-D network of ET molecules, with respect to the size and symmetry of the trihalide anions. In this manner, the role of inter-molecular interactions on the electrical properties of $(ET)_2X$ salts is studied.

The experimental sections that follow describe the synthesis, ESR results and crystal structure of $\beta$-$(ET)_2I_2Br$. Similar experimental data and results for the $\beta$-$(ET)_2X$ salts with $X = I_3^-$ and $IBr_2^-$ have been published elsewhere.[29,31,34]

## EXPERIMENTAL SECTION

### Preparations. $(n\text{-}Bu_4N)I_2Br$

Initially, 10.0g of $(n\text{-}Bu_4N)Br$ (31 mmoles) was dissolved in 200mL of boiling absolute ethanol, followed by the slow addition of 7.8g of $I_2$ (31 mmoles). The dark brown solution was hot-filtered and boiled down to 150 mL. After slow-cooling to room temperature, the solution was stored in a freezer overnight. The reddish brown needles of $(n\text{-}Bu_4N)I_2Br$ were collected, vacuum-dried, twice recrystallized from absolute ethanol and stored in a closed container in a refrigerator. Approximately 14.6g of product (91% yield) was obtained; mp 56–58°C; Analysis Calcd (Found—Midwest Microlab, Indianapolis, IN) for $(n\text{-}Bu_4N)I_2Br$: C, 33.35(33.34); H, 6.30(6.44); N, 2.43(2.61); I, 44.05(43.94).

### $\beta\text{-}(ET)_2I_2Br$

Dark distorted-hexagon shaped crystals of $\beta\text{-}(ET)_2I_2Br$ were grown by use of electrocrystallization techniques[31] in dry tetrahydrofuran at 0.8 $\mu A/cm^2$ current density (Pt electrodes) with 1.73 mM ET and 0.10 M $(n\text{-}Bu_4N)I_2Br$ at 23°C. Identical results were obtained using ET synthesized in our laboratory, or using that obtained from Strem Chemical Co. The shiny, black crystals of $\beta\text{-}(ET)_2I_2Br$ were surveyed by ESR methods,[34] which gave a peak-to-peak linewidth of ~20 G for each sample measured. Only the β-phase has been detected for $(ET)_2I_2Br$ via ESR or x-ray diffraction techniques thus far. In contrast, at least two phases of $(ET)_2I_3$[31] and $(ET)_2IBr_2$[29] have been identified, via x-ray diffraction and their ESR spectra.

### X-ray diffraction data collection and structural refinement

A flat, nearly hexagonal crystal of $\beta\text{-}(ET)_2I_2Br$ was selected for the x-ray intensity data collection experiment. On the basis of the unit cell and reflection intensity data, it was determined that $\beta\text{-}(ET)_2I_2Br$, $\beta\text{-}(ET)_2I_3$ and $\beta\text{-}(ET)_2IBr_2$ were isostructural at 298 K. The unit cell data for these three $\beta\text{-}(ET)_2X$ salts are compared at 298 K and 120 K in Table I.

Experimental details for the x-ray data collection are given in Table II. Corrections for polarization, Lorentz effects and absorption were made. Initial atomic coordinates of the ET molecule for $\beta\text{-}(ET)_2I_2Br$ were taken from a previous study of the isostructural $\beta\text{-}(ET)_2I_3$ salt.[31] All H atoms were subsequently located on a difference-Fourier map

TABLE I

Crystallographic data for the β-(BEDT-TTF)$_2$X salts with X = $I_3^-$, $I_2Br^-$, and $IBr_2^-$ at 298 K/120 K.

A. Unit cell parameters:

| | β-(BEDT-TTF)$_2$I$_3$ | β-(BEDT-TTF)$_2$I$_2$Br | β-(BEDT-TTF)$_2$IBr$_2$ |
|---|---|---|---|
| **a**(Å) | 6.615(1) / 6.561(1) | 6.612(1) / 6.613(1) | 6.593(1) / 6.589(1) |
| **b**(Å) | 9.100(1) / 9.013(2) | 9.024(2) / 8.873(2) | 8.975(2) / 8.820(2) |
| **c**(Å) | 15.286(2) / 15.173(2) | 15.192(2) / 15.100(2) | 15.093(5) / 14.988(5) |
| **α**(°) | 94.38(1) / 95.07(1) | 94.16(1) / 95.64(1) | 93.79(2) / 95.30(2) |
| **β**(°) | 95.59(1) / 95.93(1) | 95.23(1) / 95.25(1) | 94.96(2) / 94.87(2) |
| **γ**(°) | 109.78(1) / 110.28(1) | 110.12(1) / 109.79(1) | 110.54(2) / 110.28(2) |
| V(Å$^3$) | 855.9(2) / 829.2(3) | 842.3(3) / 822.4(2) | 828.7(5) / 807.1(5) |
| **\|a + b\|**(Å)[a] | 9.264(1) / 9.126(2) | 9.171(2) / 9.096(2) | 9.083(2) / 8.996(2) |

B. Unit temperature dilation of primary axes ($K^{-1} \times 10^5$) upon cooling from 298 to 120 K:[b]

| | β-(BEDT-TTF)$_2$I$_3$ | β-(BEDT-TTF)$_2$I$_2$Br | β-(BEDT-TTF)$_2$IBr$_2$ |
|---|---|---|---|
| **Δa/aΔT** | −4.6(1) | +0.1(1) | −0.3(1) |
| **Δb/bΔT** | −5.4(1) | −9.4(1) | −9.7(1) |
| **Δc/cΔT** | −4.2(1) | −3.4(1) | −3.9(1) |
| **Δ\|a + b\|/\|a + b\|ΔT** | −8.4(1) | −4.6(1) | −5.4(1) |

[a]The magnitude |a + b| is calculated from vector sum of **a** and **b**.
[b]Estimated deviations in the least significant figure are based on the observed temperature variations of ±5 degrees at 120 K.

(120 K data), with coordinates close to the calculated values (vide infra). The final reliability ratios and difference-Fourier (ΔF) map residuals are given in Table II. The non-H atom positional and equivalent thermal parameters at 298 and 120 K are listed in Table III. For comparing the H···X contact distances in β-$(ET)_2I_3$, β-$(ET)_2I_2Br$, and β-$(ET)_2IBr_2$, calculated H atom coordinates for the ethylene groups are based on C-H distances of 1.09 Å, which is the internuclear distance obtained in neutron diffraction studies.[35]

The $I_2Br^-$ anion has the inversion symmetry of space group $P\bar{1}$ imposed on it and is modelled by two superimposed components of equal probability (i.e., 50% of I-I-Br and 50% of Br-I-I). The $I_2Br^-$ anion at 298 K was initially treated as a linear rigid-body using the I-I distance of 2.919 Å in β-$(ET)_2I_3$[31] and the I-Br distance of 2.704 Å in β-$(ET)_2IBr_2$.[29] The resolution obtained with the 298 and 120 K data sets did allow for the refinement of positional and thermal parameters for terminal halide atoms individually (vide infra). A second disordered model, $Br\cdots I_2$ (i.e., with Br-I at 2.906 Å and I-I at 2.777 Å) which was observed in $CsI_2Br$,[36] gave nearly the same fit to the

TABLE II

Crystal data and refinement parameters for β-$(BEDT\text{-}TTF)_2I_2Br$ at 298 K/120 K

| | |
|---|---|
| crystal dimensions: (100 − $\bar{1}$00) 0.34 mm, (010 − 0$\bar{1}$0) 0.44 mm, (001 − 00$\bar{1}$) 0.08 mm, (110 − $\bar{1}\bar{1}$0) 0.40 mm | |
| abs. coeff. (μ at 298 K/120 K): | 39.9/40.9 $cm^{-1}$ |
| crystal density ($\rho_{calc}$ at 298 K): | 2.17 g $cm^{-3}$ |
| radiation, graphite monochromated: | $MoK_\alpha$ |
| scan mode, widths: | $2\theta-\theta$, ~ 2.5 − 3.5° |
| 2θ range (+h ±k ±l hemisphere): | $2 < 2\theta < 60°$ |
| transmission factors: | 0.32 − 0.72 |
| $R_{ave}$[a] (298 K/120 K data): | 0.02/0.01 |
| intensity data, observed (298 K/120 K): | 5474/5191 |
| unique (NO): | 4514/4509 |
| no. parameters (NV) varied: | 178 |
| max. residuals on final dif.-Fourier:[b] | 4.1/1.5 e-/Å$^3$ |
| R(F)[c] (298 K/120 K) | 0.057/0.042 |
| wR(F)[d] | 0.045/0.046 |
| GOF[e] | 2.44/1.79 |

[a] $R_{ave} = \Sigma|F_{ij}^2 - F_i^2|/F_{ij}^2$; with 398/494 terms having multiple observations at 298 K/120 K, respectively.

[b] The largest peaks were in the vicinity of the $I_2Br^-$ rigid body.

[c] $R(F) = \Sigma|F_o - kF_c|/\Sigma F_o$.

[d] $wR(F) = [\Sigma w(F_o - kF_c)^2/\Sigma wF_o^2]^{1/2}$. Variances are: $\sigma^2(F_o) = \sigma_c^2(F_o) + [0.04(F_o)^2]^2$, where $\sigma_c^2(F_o)$ values were from counting statistics alone.

[e] $GOF = [\Sigma w(F_o - kF_c)^2/(NO - NV)]^{1/2}$, for NO observations and NV variable parameters.

reflection data, but this model was rejected because the observed electron density at the I(2)/Br site was "pear-shaped" and indicated that the heavier atom [I(2)] was further from the inversion center than the lighter atom [Br]. The geometry $(I\text{-}Br\text{-}I)^-$ has not been observed in any crystal structure to date[37] and was not the case here, based on the observed difference density synthesis. In fact, the atom of highest atomic number always occupies the central position in trihalide anions.[37] In alternate least-squares cycles, the positional and thermal parameters for the terminal I(2) or Br atom were varied, along with all parameters for the C and S atoms (see Table III), until convergence was reached. The "shift/error" ratios were less than 0.1 on the final cycles of refinement except for some $U_{ij}$ for I(2) and Br, which were less than 0.2. The thermal motions of atoms of the $I_2Br^-$ anion have the largest components at right angles to the vector along the length of the anion, and hence did not indicate translational disorder along the I-I or I-Br vector. Similar directions for the largest component of thermal motion were also observed in the symmetrical trihalide anions of β-$(ET)_2IBr_2$[29] and β-$(ET)_2I_3$.[31] The thermal parameters for all terminal ethylene C atoms are large at 298 K, but are considerably less, especially for the C(9)-C(10) group at 120 K (see Table III). As an additional note, the thermal motions of the ethylene groups of the ET molecule of β-$(ET)_2I_2Br$ are nearly identical to those of β-$(ET)_2IBr_2$,[29] both at 298 K and at 120 K.

The crystal structures of β-$(ET)_2X$, X = $I_2Br^-$ and $IBr_2^-$, are more accurately described by the atomic parameters derived at 120 K, rather than 298 K, since no significant orientational disorder is observed for the ethylene groups at the lower temperature. However, the disorder that remains in β-$(ET)_2I_2Br$, even at 120 K, is that which is imposed by the space group on the asymmetric $I_2Br^-$ anion.

As shown by the intramolecular bond lengths and angles at 298 K in Table IV, the intramolecular S-C (ethyl) and C-C double bond distances in β-$(ET)_2I_2Br$ are normal when compared to the average S-C and C-C distances of 1.77(1) and 1.44(1) Å, respectively, that are derived from ordered ET molecules in other ET:X salts.[23-25,33] However, the geometries of the two ethylene groups at 298 K (see Table IV) are distorted as a result of some disorder. In β-$(ET)_2I_3$, two distinct sites are resolved for the C(9)-C(10) ethylene group which coexist with a structural modulation below ~195 K (vide infra).[38,41] The positions of this ethylene group in the β-$(ET)_2X$ salts with X = $I_2Br^-$ or $IBr_2^-$ at 298 K are the average positions of these two sites in β-$(ET)_2I_3$ at 120 K.

TABLE III

Final atomic positional and equivalent isotropic thermal parameters[a] for β-$(ET)_2I_2Br$ at 298/120 K

| Atom | X | Y | Z | $U_{eq}$ |
|---|---|---|---|---|
| I(1) | 0.0000 | 0.0000 | 0.0000 | 0.577(2) |
| | 0.0000 | 0.0000 | 0.0000 | 0.287(2) |
| I(2) | 0.3936(2) | 0.2593(1) | −0.0150(1) | 0.739(4) |
| | 0.3914(1) | 0.2634(1) | −0.0178(1) | 0.314(3) |
| Br | −0.3682(2) | −0.2446(1) | 0.0133(1) | 0.692(4) |
| | −0.3614(1) | −0.2433(1) | 0.0169(1) | 0.252(1) |
| S(1) | 0.4640(2) | −0.2605(3) | 0.4480(1) | 0.471(4) |
| | 0.4648(1) | −0.2600(1) | 0.4485(1) | 0.226(4) |
| S(2) | 0.0994(2) | −0.1459(1) | 0.4288(1) | 0.504(4) |
| | 0.0971(1) | −0.1453(1) | 0.4275(1) | 0.246(4) |
| S(3) | 0.2803(2) | −0.4298(1) | 0.6205(1) | 0.438(3) |
| | 0.2820(1) | −0.4270(1) | 0.6208(1) | 0.212(4) |
| S(4) | −0.0816(2) | −0.3120(1) | 0.5993(1) | 0.457(3) |
| | −0.0840(1) | −0.3095(1) | 0.5988(1) | 0.225(4) |
| S(5) | 0.6446(2) | −0.1378(2) | 0.2869(1) | 0.660(5) |
| | 0.6447(1) | −0.1425(1) | 0.2864(1) | 0.301(4) |
| S(6) | 0.2132(2) | 0.0029(2) | 0.2655(1) | 0.737(5) |
| | 0.2100(1) | 0.0015(1) | 0.2637(1) | 0.352(5) |
| S(7) | 0.1978(2) | −0.5377(1) | 0.7964(1) | 0.570(4) |
| | 0.1993(1) | −0.5334(1) | 0.7973(1) | 0.294(4) |
| S(8) | −0.2372(2) | −0.3965(1) | 0.7703(1) | 0.571(4) |
| | −0.2434(1) | −0.3954(1) | 0.7693(1) | 0.257(4) |
| C(1) | 0.2295(6) | −0.2528(4) | 0.4875(2) | 0.352(12) |
| | 0.2266(4) | −0.2524(4) | 0.4872(2) | 0.188(14) |
| C(2) | 0.1509(6) | −0.3249(4) | 0.5595(2) | 0.364(12) |
| | 0.1497(4) | −0.3238(4) | 0.5589(2) | 0.189(14) |
| C(3) | 0.4422(6) | −0.1590(4) | 0.3561(2) | 0.376(12) |
| | 0.4423(4) | −0.1610(4) | 0.3552(2) | 0.195(14) |
| C(4) | 0.2758(6) | −0.1049(4) | 0.3471(2) | 0.398(13) |
| | 0.2730(4) | −0.1066(4) | 0.3460(2) | 0.196(14) |
| C(5) | 0.1181(6) | −0.4506(4) | 0.7075(2) | 0.342(12) |
| | 0.1177(4) | −0.4481(4) | 0.7072(2) | 0.174(13) |
| C(6) | −0.0477(6) | −0.3960(4) | 0.6974(2) | 0.338(12) |
| | −0.0513(4) | −0.3945(3) | 0.6967(2) | 0.162(13) |
| C(7) | 0.6313(7) | 0.0265(6) | 0.2323(4) | 0.678(19) |
| | 0.6340(5) | 0.0296(4) | 0.2348(2) | 0.262(16) |
| C(8) | 0.4181(8) | 0.0216(7) | 0.1939(4) | 0.829(23) |
| | 0.4098(5) | 0.0084(4) | 0.1883(2) | 0.289(17) |
| C(9) | 0.0313(10) | −0.5015(10) | 0.8791(4) | 1.276(36) |
| | 0.0467(6) | −0.4787(5) | 0.8818(2) | 0.382(20) |
| C(10) | −0.1810(10) | −0.5146(9) | 0.8505(4) | 1.170(31) |
| | −0.1932(6) | −0.5240(5) | 0.8474(3) | 0.365(20) |

[a]The equivalent temperature factor is $1/3\ \Sigma_i\Sigma_j\ [U_{ij}a_ia_ja_i{}^*a_j{}^*]$. Estimated standard deviations are enclosed in parentheses.

TABLE IV

Final distances (Å) and angles (°) for β-(ET)$_2$I$_2$Br at 298/120 K[a]

| Bond | Distance | Bonds | Angle |
|---|---|---|---|
| S(1)-C(1) | 1.734(3)/1.748(3) | C(1)-S(1)-C(3) | 95.3(2)/95.4(1) |
| S(1)-C(3) | 1.746(4)/1.751(3) | C(1)-S(2)-C(4) | 95.5(2)/95.8(1) |
| S(2)-C(1) | 1.739(4)/1.741(3) | C(2)-S(3)-C(5) | 95.3(2)/95.3(1) |
| S(2)-C(4) | 1.752(4)/1.749(3) | C(2)-S(4)-C(6) | 95.2(2)/95.2(1) |
| S(3)-C(2) | 1.739(4)/1.743(3) | C(3)-S(5)-C(7) | 100.8(2)/99.8(2) |
| S(3)-C(5) | 1.757(3)/1.756(3) | C(4)-S(6)-C(8) | 103.6(2)/103.2(2) |
| S(4)-C(2) | 1.739(3)/1.747(3) | C(5)-S(7)-C(9) | 101.2(2)/100.2(2) |
| S(4)-C(6) | 1.751(3)/1.753(3) | C(6)-S(8)-C(10) | 101.5(2)/101.3(2) |
| S(5)-C(3) | 1.744(3)/1.742(3) | C(2)-C(1)-S(1) | 123.0(3)/122.4(2) |
| S(5)-C(7) | 1.774(5)/1.801(4) | C(2)-C(1)-S(2) | 121.8(3)/122.7(2) |
| S(6)-C(4) | 1.735(4)/1.744(3) | S(2)-C(1)-S(1) | 115.2(2)/114.9(2) |
| S(6)-C(8) | 1.785(5)/1.810(4) | C(1)-C(2)-S(3) | 122.7(3)/123.0(2) |
| S(7)-C(5) | 1.741(4)/1.750(3) | C(1)-C(2)-S(4) | 122.1(3)/121.7(2) |
| S(7)-C(9) | 1.827(5)/1.822(4) | S(3)-C(2)-S(4) | 115.1(2)/115.2(2) |
| S(8)-C(6) | 1.745(3)/1.748(3) | C(4)-C(3)-S(1) | 117.4(3)/116.9(2) |
| S(8)-C(10) | 1.771(5)/1.805(4) | C(4)-C(3)-S(5) | 127.7(3)/128.1(3) |
| C(1)-C(2) | 1.365(5)/1.359(4) | S(5)-C(3)-S(1) | 114.9(2)/114.9(2) |
| C(3)-C(4) | 1.348(5)/1.363(4) | C(3)-C(4)-S(2) | 116.4(3)/116.6(3) |
| C(5)-C(6) | 1.349(5)/1.359(4) | C(3)-C(4)-S(6) | 128.6(3)/128.4(3) |
| C(7)-C(8) | 1.460(7)/1.525(5) | S(6)-C(4)-S(2) | 115.0(2)/114.9(2) |
| C(9)-C(10) | 1.393(8)/1.526(5) | C(6)-C(5)-S(3) | 116.6(3)/116.8(2) |
| I(1)-I(2) | 2.881(2)/2.901(2) | C(6)-C(5)-S(7) | 128.8(3)/128.6(3) |
| I(1)-Br | 2.701(2)/2.680(2) | S(7)-C(5)-S(3) | 114.6(2)/114.6(2) |
| | | C(5)-C(6)-S(4) | 117.2(3)/117.0(2) |
| | | C(5)-C(6)-S(8) | 128.6(3)/128.7(3) |
| | | S(8)-C(6)-S(4) | 114.3(2)/114.2(2) |
| | | C(8)-C(7)-S(5) | 117.8(3)/113.9(3) |
| | | C(7)-C(8)-S(6) | 118.5(4)/114.4(3) |
| | | C(10)-C(9)-S(7) | 118.4(5)/112.9(3) |
| | | C(9)-C(10)-S(8) | 121.2(5)/112.9(3) |

[a]Estimated standard deviations are enclosed in parentheses.

### ESR results

The ambient pressure ESR experiments used a thin plate sample of β-(ET)$_2$I$_2$Br with dimensions 450 × 400 × 170 micrometers placed in a rectangular microwave cavity at 9.8 GHz. The ESR lineshape was Dysonian[39] from 2 to 300 K, and could be accurately characterized at all temperatures by a linear combination of Lorenzian absorption and dispersion. The static magnetic field was applied approximately normal to the broad sample face, and the microwave magnetic field was roughly in the plane for the ESR measurements. The peak-to-peak linewidth of the absorption part of the ESR signal decreases with decreasing temperature from 19.3(5) Oe at 300 K to 2.7(1) Oe at 5 K, then increases very slightly between 5 and 2 K.

Using a thin plate calculation[40] for resonance in metallic samples, the spin susceptibility corrected for microwave skin depth plus the skin depth/plate thickness ratio were obtained from the ESR signal. As shown in Figure 1, the spin susceptibility is independent of temperature from 2 to 300 K at $1.5 \times 10^{-3}$ emu/mole within a relative experimental uncertainty of 25%, indicative of the Pauli spin paramagnetism of a metal. Also shown in Figure 1 is the microwave conductivity calculated from the skin depth/sample thickness ratio. This conductivity rises with decreasing temperature from 300 to 15 K, then appears to saturate near 200 $(\text{ohm-cm})^{-1}$ at lower temperatures. This "saturation" may reflect the use of a thin plate calculation[40] for ESR in this sample whose thickness is nearly one-half the cross-sectional dimensions, far from a true thin plate geometry. Hence the microwave conductivity shown in Figure 1 should be confirmed by 4-probe conductivity measurements below 25 K when large enough crystals become available. The strongly Dysonian ESR lineshape observed below 30 K indicates that the microwave conductivity is large in at least two directions for β-$(ET)_2I_2Br$ with one direction in the plane of the thin sample.

Low field ESR measurements were also performed on the same sample as the microwave measurements at a resonant field of 10 Oe.

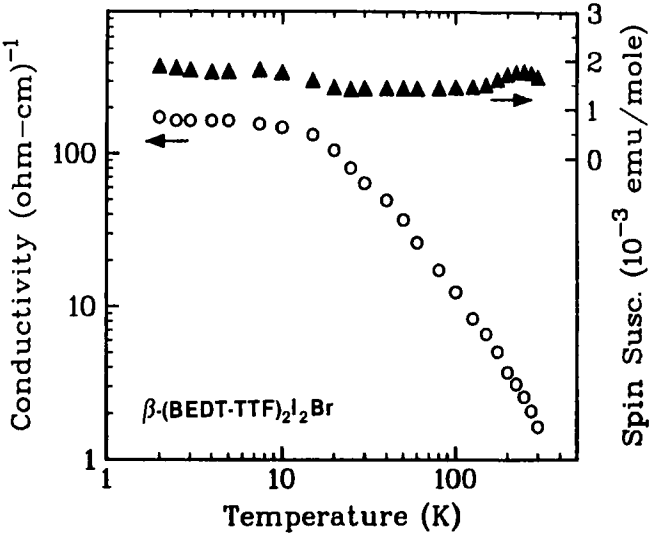


FIGURE 1 Spin susceptibility corrected for microwave skin depth and the depth/plate ratio for β-$(ET)_2I_2Br$. The calculated microwave conductivity (see Text) is also included.

We find that the peak-to-peak linewidth at low field is somewhat larger than at microwave frequencies, on the oder of 10 Oe. The temperature dependence of the spin susceptibility at low field is consistent with that at microwave frequencies, i.e., the susceptibility is independent of temperature. We did not observe any evidence for superconductivity (i.e., the complete disappearance of the ESR signal) at ambient pressure and at a pressure of up to 5 kbar (1.07 K $< T <$ 4 K). Using rf penetration depth measurements, we do not observe superconductivity down to 0.45 K at ambient pressure.

## DISCUSSION

As shown in Table I, the dilations of the crystallographic axes of β-(ET)$_2$I$_2$Br are nearly identical to those of β-(ET)$_2$IBr$_2$. Therefore, the crystal packing forces in β-(ET)$_2$I$_2$Br in the temperature range 298–120 K may closely resemble those of β-(ET)$_2$IBr$_2$. In contrast, the isostructural β-(ET)$_2$I$_3$ undergoes a structural phase transition[38,41] at ~ 195 K. Note that the largest dilation is along [110] (**a** + **b**) for all three salts (see Table I). The structural consequences of the anion size differences for X = $I_3^-$, $I_2Br^-$, and $IBr_2^-$ are directly measurable in the translational vector magnitude |**a** + **b**| (see Table I), whose direction is nearly parallel to the long axis of the anion. The decrease in the |**a** + **b**| distance is rather constant at ~0.087(2) Å per each atom substitution of Br for I in this trihalide series at 298 K. This contraction is expected to involve some shortening of the distance between cations that stack along the [110] direction, but this depends on the orientation of the cation planes with the stacking axis (vide infra). For the *inter*stack spacings along [100], much smaller decreases are observed (~0.007(2) Å) per each atom substitution of Br for I. Thus, both the thermal expansion of the lattice *and* the halide substitution (i.e., I for Br) are expected to have a significant role in determining the inter-cation interactions, and (ultimately) the electrical behavior of these β-(ET)$_2$X salts.

The variation of the S···S contacts will be discussed below with special attention given to those that are in the *ab* plane. An *overall* contraction of the S···S contacts along the [100] and [1–10] directions is observed for decreasing anion size. The interstack S···S contacts less than 3.60 Å ($d_1$-$d_6$) are shown in Figure 2 and are listed in Table V for the isostructural β-(ET)$_2$X salts (X = $I_3^-$, $I_2Br^-$, $IBr_2^-$), and a plot of the average S···S contacts along [100] and [1–10] versus unit cell volume in these salts is given in Figure 3. To accurately char-

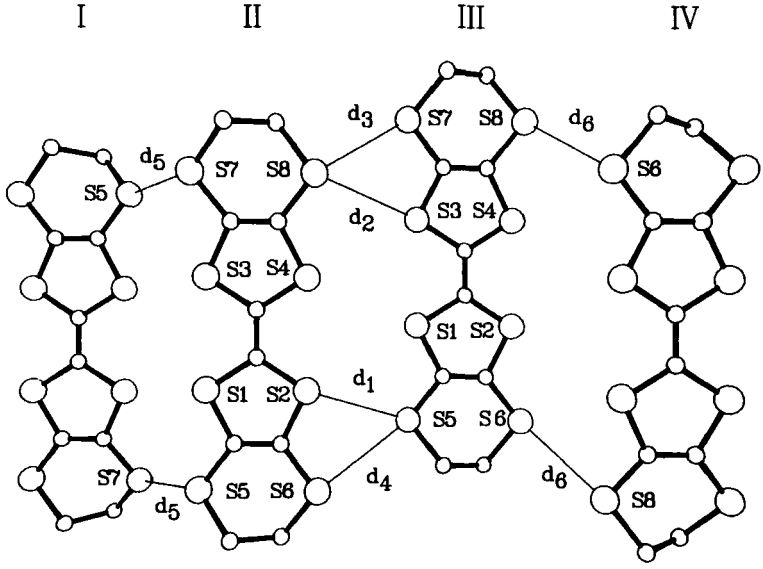


FIGURE 2 A perspective view of the four ET molecules that comprise the interstack network in each β-$(ET)_2X$ salt. The interstack S···S contacts, $d_1$-$d_6$, are indicated by thin lines. For clarity, H atoms are removed. Arbitrary thermal ellipsoids were used.

acterize the interstack S···S contacts along [100] and [1–10], the average of the *shortest* contacts (≤ 3.55 Å at 120 K) along a given direction are chosen for the plot in Figure 3. The result of either decreasing the temperature or substituting a smaller anion is, as predicted, a decrease in the interstack S···S contacts on the average. Thus, the observed metallic properties of these three salts from 298 to 120 K are accompanied by large differences in anion length (10.14 Å for X = $I_3^-$ to 9.30 Å for X = $IBr_2^-$), unit cell volume (856 $Å^3$ for X = $I_3^-$ at 298 K to 807 $Å^3$ for X = $IBr_2^-$ at 120 K), and S···S network geometry (the shortest average contacts range from 3.50 to 3.61 Å). Further structural details that compare the significant intra- and interstack S···S contacts within the three salts are presented in the next section.

### Correlations between anion size and the S···S contacts

Recent molecular orbital calculations[42] have shown that the intrastack S···S interactions (along [110]) contribute significantly to the overlap integral and vary systematically with anion size. As shown in Figure 3 and Table V, the *inter*stack contact distances also correlate with anion size or unit cell volume. These S···S distances define the 2-D

TABLE V

Intermolecular S···S distances for β-(BEDT-TTF)$_2$X (X = $I_3^-$, $I_2Br^-$, $IBr_2^-$) at 298 K and 120 K

| | Interstack contact | | β-(ET)$_2$I$_3$ distance[a] | β-(ET)$_2$I$_2$Br distance | β-(ET)$_2$IBr$_2$ distance |
|---|---|---|---|---|---|
| d1 | S(5)···S(2) | (~*a*)[b]298 K | 3.574(2)[c] | 3.562(3) | 3.559(2) |
| | | 120 K | 3.555 ± 0.033 | 3.522(1) | 3.514(2) |
| | | difference | 0.019 | 0.040 | 0.045 |
| d2 | S(3)···S(8) | (~*a*)298 K | 3.651(1) | 3.656(3) | 3.652(2) |
| | | 120 K | 3.577 ± 0.026 | 3.602(1) | 3.593(2) |
| | | difference | 0.074 | 0.054 | 0.59 |
| d3 | S(7)···S(8) | (~*a*)298 K | 3.598(2) | 3.578(3) | 3.560(2) |
| | | 120 K | 3.534 ± 0.022 | 3.548(1) | 3.510(2) |
| | | difference | 0.064 | 0.030 | 0.050 |
| d4 | S(5)···S(6) | (~*a*)298 K | 3.600(2) | 3.585(3) | 3.593(2) |
| | | 120 K | 3.551 ± 0.048 | 3.579(1) | 3.551(2) |
| | | difference | 0.049 | 0.006 | 0.042 |
| d5 | S(5)···S(7) | (~*a-b*)298 K | 3.628(2) | 3.615(3) | 3.572(2) |
| | | 120 K | 3.548 ± 0.033 | 3.530(1) | 3.498(2) |
| | | difference | 0.080 | 0.084 | 0.074 |
| d6 | S(6)···S(8) | (~*b*)298 K | 3.593(2) | 3.585(3) | 3.564(2) |
| | | 120 K | 3.552 ± 0.098 | 3.515(2) | 3.504(2) |
| | | difference | 0.041 | 0.070 | 0.060 |
| Shortest Intrastack Distances | | | | | |
| | S(1)···S(4) | (~*ab*)298 K | 3.806(2) | 3.788(3) | 3.772(2) |
| | | 120 K | 3.725 ± 0.038 | 3.751(1) | 3.730(2) |
| | | difference | 0.081 | 0.037 | 0.042 |
| | S(2)···S(3) | (~*ab*)298 K | 3.775(2) | 3.762(2) | 3.748(2) |
| | | 120 K | 3.721 ± 0.019 | 3.729(1) | 3.723(2) |
| | | difference | 0.054 | 0.033 | 0.025 |
| | S(3)···S(4) | (~*ab*)298 K | 3.758(1) | 3.778(3) | 3.795(2) |
| | | 120 K | 3.696 ± 0.018 | 3.714(1) | 3.730(2) |
| | | difference | 0.062 | 0.064 | 0.065 |

[a]Each distance in the modulated structure of β-(ET)$_2$I$_3$ at 120 K is an average value accompanied by the range allowed by the modulation. The differences are those between 298 and 120 K values.

[b]The ~*a-b*, ~*a* and ~*b* directions apply to *inter*-stack interactions within the 2-D network cations. The *intra*-stack direction is along *ab*, where distances less than 3.6 Å are not found at either temperature.

[c]Estimated standard deviations are enclosed in parentheses, and are ±0.003 to ±0.005 Å for the average distances at 120 K for β-(ET)$_2$I$_3$.

network of ET molecules and are generally 0.1–0.2 Å shorter than the intrastack contacts. As shown in Table V, the *inter*stack S···S contacts for β-(ET)$_2$I$_2$Br at 120 K are always longer than those for β-(ET)$_2$IBr$_2$. The S···S contacts along [100] for β-(ET)$_2$I$_3$ at 120 K do not strictly follow the trend. This may be a consequence of the structural modulation that permits displacements of ET molecules on the order of ±0.09 Å.

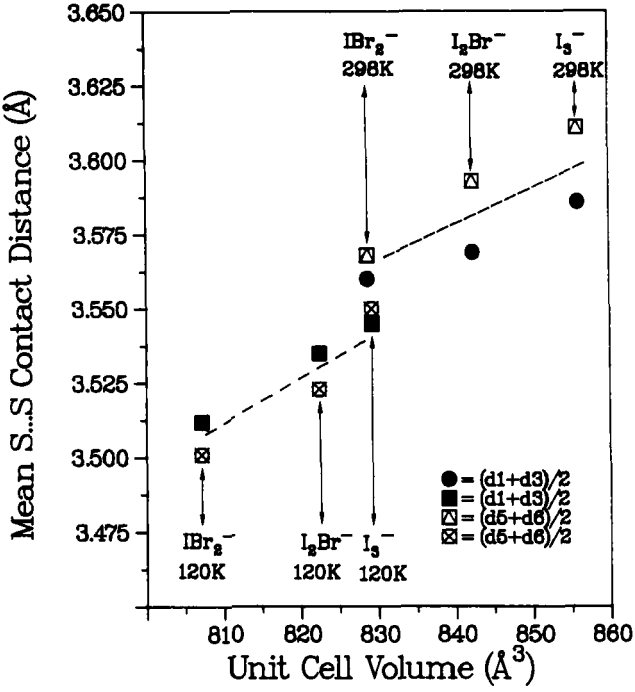


FIGURE 3 Plot of the average of the shortest two interstack S···S contact distances which are $d_1$ and $d_3$ along [100] and $d_5$ and $d_6$ along [1–10], at 298 and 120 K versus unit cell volume for the β-$(ET)_2X$ salts, X = $I_3^-$, $I_2Br^-$, $IBr_2^-$.

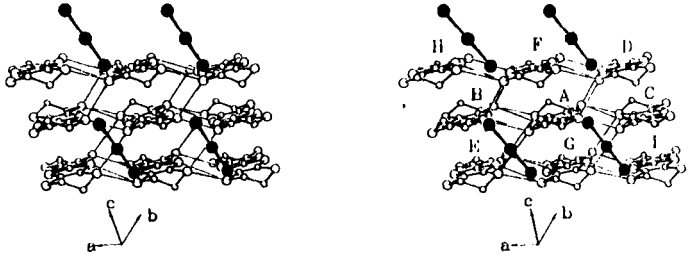


FIGURE 4 A stereoview of the interstack "sheet-like network" of the ET molecules and the adjacent anion sheet viewed along the long in-plane axis of the ET molecule. The locations of the ET molecules: A(x,y,z); B(x + 1,y,z); C(x − 1,y,z); D(1 − x, − y,1 − z); E( − x, − y,1 − z); F(1 − x, − y,1 − z); G( − x, − 1 − y,1 − z); H(2 − x, − y,1 − z) and I( − 1 − x, − 1 − y,1 − z). The H atoms have been removed for clarity. All trihalide anions are located on inversion centers, and form planes which alternate with the 2D sheets of ET molecules in a direction that is perpendicular to the *ab* plane.

As shown in Figure 3, the unit cell volume variations parallel the incremental differences in length of these trihalide anions (including van der Waals radii) which are ~0.42 Å for $IBr_2^-$ to $I_2Br^-$ and ~0.42 Å for $I_2Br^-$ to $I_3^-$. The vector along the length of the trihalide ion is nearly parallel to the stacking axis of the cations ([110]) for each of the isostructural β-(ET)$_2$X salts. This is the direction which also relates the ET molecules that are labelled "G" and "F" in Figure 4. The interstack S···S distances that have large directional components parallel to this "anion vector" (i.e., ~[$\bar{1}$10]) are d5 and d6 and these contacts expand more than those in other directions upon substitution of a longer anion in this lattice (see Table V). The [110] components of the interplanar (ET) spacings are listed in Table VI as ΔZ, and are calculated from a local Cartesian coordinate system for the six neighboring cations to the ET molecule labelled "A" in the center of Figure 4. Except for the widest ΔZ separation (between molecules A-F), these values are rather constant versus increasing anion length. Apparently, the S···S contacts directed along [100], i.e., d1-d4, and the intrastack spacing between molecules "A" and "G" (Figure 4) are not noticeably affected by the substitution of larger anions.

Another parameter which measures the effect of anion size on the ET network is the intercation dihedral angle (ϕ) for nearest-neighbor ET planes, which is defined by the relation, $\phi = \tan^{-1}(\Delta Z/\Delta X)$. Based on the ϕ angles in Table VI, the overall packing of ET molecules in the superconductor β-(ET)$_2$IBr$_2$ is approximately the same as the packing in β-(ET)$_2$I$_2$Br, for which superconductivity has not been observed even under modest pressure.[43] Thus, the minor differences in the S···S framework are apparently not as important as the presence of anion order, or disorder, in determining superconductivity in β-(ET)$_2$X salts.

Another correlation may involve interactions between cation and anion via H···X contacts, but significant differences in these distances are *not* observed. In analyzing H···X interaction distances in the β-(ET)$_2$X salts, one must consider two features: 1) the presence of correlated site-occupancies and positions in the ET ethylene groups because of the structural modulation[38,41] observed in β-(ET)$_2$I$_3$ at 120 K; and 2) the presence of two sets of contact distances for H···X interactions for β-(ET)$_2$I$_2$Br at 120 K, i.e., involving either I or Br, which are the terminal atoms of the anion. The above features are thus a function of anion size and long-range order. The possible H···I and H···Br contacts (calculated) less than 3.2 Å at 120 K for the β-(ET)$_2$X salts (X = $I_3^-$, $I_2Br^-$ and $IBr_2^-$) are listed in Table VII. Upon the inclusion of different trihalide anions into the "cavity"

TABLE VI

Some inter-cation packing interaction distances and angles within the sheetlike network of cations for β-(BEDT-TTF)$_2$X, X = $I_3^-$, $I_2Br^-$, $IBr_2^-$ at 120 K

| Symmetry of second[a] molecule | ET label (Figure4) | ΔY shift (long in-plane axis) | | | ΔZ shift (out of molecular plane) | | | ϕ $\tan^{-1}\Delta Z/\Delta X$ (intermolecular angle) | | |
|---|---|---|---|---|---|---|---|---|---|---|
| | | $I_3$ | $I_2Br$ | $IBr_2$ | $I_3$ | $I_2Br$ | $IBr_2$ | $I_3$ | $I_2Br$ | $IBr_2$ |
| X+1,Y,Z | (B,C) | 1.81 | 1.90 | 1.88 | 1.46 | 1.40 | 1.29 | 13.4 | 12.8 | 12.7 |
| −X+1,−Y−1,−Z+1 | (D) | 0.18 | 0.25 | 0.27 | 1.83 | 1.90 | 1.92 | 16.3 | 17.1 | 17.2 |
| −X,−Y−Z+1 | (E) | 2.15 | 2.00 | 1.93 | 2.44 | 2.48 | 2.45 | 23.1 | 23.8 | 23.5 |
| −X+1,−Y,−Z+1 | (F) | 3.96 | 3.89 | 3.81 | 3.91 | 3.88 | 3.85 | 84.0 | 81.9 | 82.2 |
| −X,−Y−1,−Z+1 | (G) | 1.63 | 1.65 | 1.61 | 3.30 | 3.31 | 3.30 | 88.1 | 89.6 | 89.6 |

[a]All distances are in Ångstrom units (±0.01 Å) from the central molecule (X,Y,Z), or "A" in Figure 4, to molecule "B" through "G" in Figure 4, and are based on orthogonal coordinates described by X along the short in-plane molecular axis [S(1) → S(2)], Y along the long in-plane molecular axis [S(1) → S(3)] and Z normal to the plane defined by the X and Y vectors, with the origin at the midpoint of the C(1)═C(2) bond. The average structure at 120 K of β-(BEDT-TTF)$_2$I$_3$ is used here.

TABLE VII

Calculated cation-anion contacts for the β-(ET)$_2$X salts X = $IBr_2^-$, $I_2Br^-$, and $I_3^-$

| X···H distance < 3.2 Å | H-atom symmetry | Br only Distance in β-(ET)$_2$IBr$_2$ | I/Br Distance in β-(ET)$_2$I$_2$Br | I only Distance in β-(ET)$_2$I$_3$ |
|---|---|---|---|---|
| I(1)···H81 | 1[a] | 3.23 | 3.27 | 3.29 ± .03[c] |
| I(2) − or −Br···H(102)[b] | 2 | 2.91 | 2.83/3.03 | 2.83 ± .20 |
| I(2) − or −Br···H(81) | 1 | 2.92 | 3.04/2.97 | 3.04 ± .02 |
| I(2) − or −Br···H(101)[b] | 3 | 2.94 | 3.00/3.02 | 3.00 ± .28 |
| I(2) − or −Br···H(82) | 4 | 3.18 | 3.16/3.22 | 3.21 ± .09 |
| X···S distance < 4.0 Å | | | | |
| I(2) − or −Br···S(7) | 5 | 3.761 | 3.810/3.862 | 3.922 |

Approximate van der Waals radii sums:[d] I-H (3.3Å) Br-S (3.8Å) I-S (3.9Å) Br-H (3.2Å)

[a]Symmetries for contacted H atoms are (1) x,y,z (2) 1+x, 1+y, z−1 (3) −x, −y, 1−z (4) 1−x, −y, −z

[b]For β-(ET)$_2$I$_3$, the X···H distances for the isostructural component, B, of the disordered ethylene groups are included.

[c]The range of allowed X···H distances from the average within the modulated structure are also given.

[d]See reference 20 for a compilation of van der Waals radii.

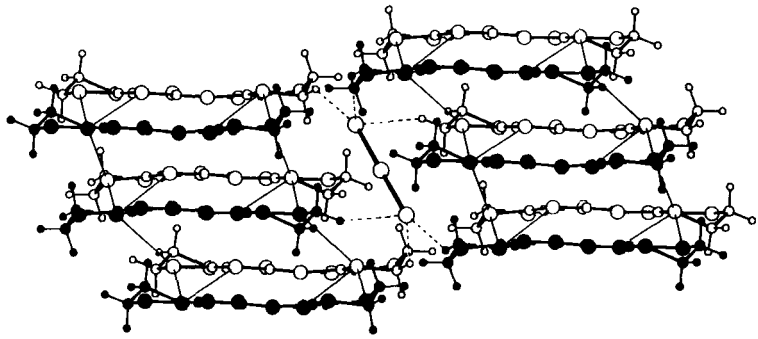

FIGURE 5 A projection view of the cation-anion H···X interactions (broken lines) between the trihalide anion in β-(ET)$_2$X, X= $I_3^-$, $I_2Br^-$, or $IBr_2^-$, at 120 K. Thin lines represent the S···S contacts $d_1$-$d_6$ (see Table V). The view is along the short in-plane axis of the ET molecule with the long in-plane axis along the horizontal.

composed of H-atoms from the ethylene groups of 2-D ET networks, the crystal packing interactions that result (i.e., H···I or H···Br) are expected to be different. One must also consider the increase in H-bonding strength in the series Cl > Br > I. However, the shortest H···X contacts are similar in all three cases, and involve H(102), H(81), and H(102′) (see Table VII). The presence of these *three* H···X distances (see Figure 5), which are on the order of 3.0 Å (see Table VII), appears to be a constant feature which involves both ethylene groups of the ET molecule. Even though the I(2)-I(1) and Br-I(1) distances vary by 0.22 Å in β-$(ET)_2I_2Br$, three short (d< 3.0(1) Å) H···X distances remain. In other words, the approximate H···X interaction distance for either the X = I(2) or X = Br atom is on the order of 3.0(1) Å, regardless of the lattice-imposed disorder of the $(I\text{-}I\text{-}Br)^-$ anion. The inversion symmetry at the anion site makes the distinction between H···I and H···Br impossible for β-$(ET)_2I_2Br$. The mean H···Br distance of ~ 2.92(2) Å for three of the contacts in β-$(ET)_2IBr_2$ at 120 K best typifies the approximately trigonal coordination (see Figure 5). The next closest calculated H···X contact in each case is ~0.25 Å longer. Finally, to complete the description of significant cation-anion distances, the closest X···S contacts are included in Table VII and are observed to be equal to or greater than the associated van der Waals radii sum[20] for all three of the above β-$(ET)_2X$ salts. Therefore, X···S contacts are likely of secondary importance for cation-anion interactions, compared to the H···X contacts.

## CONCLUSION

On the basis of the ESR measurements, crystals of β-$(ET)_2I_2Br$ remain metallic upon cooling to 1.07 K, but this organic metal never becomes superconducting, even under applied hydrostatic pressure of up to 5 kbar at 4 K < T < 1.07 K. The lack of superconductivity in this salt down to 0.45 K is verified by rf penetration depth measurements. Thus, in spite of the nearly identical structural features of these three strictly isostructural salts, which includes ET molecular packing, S···S contacts in the ET network, and cation-anion contacts, the electrical behavior of β-$(ET)_2I_2Br$ is drastically different from that of β-$(ET)_2I_3$ and β-$(ET)_2IBr_2$, which are ambient pressure superconductors. Therefore, without significant changes in these structures except that the $I_2Br^-$ anion is disordered in β-$(ET)_2I_2Br$, it appears that *anion disorder* is responsible for the observed lack of

superconductivity in β-(ET)$_2$I$_2$Br. This suggests that future superconductors in the β-(ET)$_2$X system will likely result from the incorporation of linear-centrosymmetric anions in the lattice.

## REGISTRY NUMBERS

ET: 66946-48-3
β-(BEDT-TTF)$_2$I$_2$Br: 96164-65-7
(n-Bu)$_4$N$^+$I$_2$Br$^-$: 3419-99-6

## SUPPLEMENTARY MATERIAL AVAILABLE

Tables of the observed and calculated structure factors, least-squares planes, calculated hydrogen coordinates and the non-H atom anisotropic thermal parameters for β-(ET)$_2$I$_2$Br at 298 K and 120 K and atomic positional and thermal parameters for β-(ET)$_2$IBr$_2$ at 120 K (47 pages) are available. Ordering information is given on any current masthead page.

### Acknowledgment

Work at Argonne National Laboratory is under Contract W-31-109-Eng-38 and at Sandia National Laboratory under Contract KC020202 with the U.S. Department of Energy (DOE), Office of Basic Energy Sciences, Division of Materials Sciences. We wish to thank D. L. Overmyer for his technical assistance.

### References

1. K. Bechgaard, *Mol. Cryst. Liq. Cryst.*, **79**, 1 (1982).
2. B. Liautard, S. Peytavin, G. Brun and M. Maurin, *J. Phys. (Paris), Colloque C3, Supplement 6*, **44**, C3-951 (1983).
3. K. Bechgaard, K. Carneiro, F. B. Rasmussen, M. Olsen, G. Rindorf, C. S. Jacobsen, H. J. Pedersen and J. C. Scott, *J. Am. Chem. Soc.*, **103**, 2440 (1981).
4. S. S. P. Parkin, D. Jerome and K. Bechgaard, *Mol. Cryst. Liq. Cryst.*, **79**, 213 (1982).
5. D. Jerome, A. Mazaud, M. Ribault and K. Bechgaard, *J. Phys. (Paris) Lett.*, **41**, L95 (1980).
6. M. Ribault, J. P. Pouget, D. Jerome and K. Bechgaard, *J. Phys. (Paris) Lett.*, **41**, L610 (1980).
7. S. S. P. Parkin, F. Creuzet, M. Ribault, D. Jerome, K. Bechgaard and J. M. Fabre, *Mol. Cryst. Liq. Cryst.*, **79**, 249 (1982).
8. R. Moret, J. P. Pouget, R. Comes and K. Bechgaard, *J. Phys. (Paris), Colloque C3, Supplement 6*, C3–957 (1983).

9. C. S. Jacobsen, H. J. Pedersen, K. Mortensen, G. Rindorf, N. Thorup, J. B. Torrance and K. Bechgaard, *J. Phys.: Solid State Physics*, **15**, 2651 (1982).
10. K. Mortensen, Y. Tomkiewicz, T. D. Schultz and E. M. Engler, *Phys. Rev. Lett.*, **46**, 1234 (1981).
11. S. Tomic, D. Jerome, P. Monod and K. Bechgaard, *J. Phys. (Paris), Colloque C3, Supplement 6*, **44**, C3–1083 (1983).
12. J. P. Pouget, R. Moret, R. Comes, K. Bechgaard, J. M. Fabre and L. Giral, *Mol. Cryst Liq. Cryst.*, **79**, 129 (1982).
13. R. H. Friend and D. Jerome, *J. Phys. C: Solid State Phys.*, **12**, 1441 (1979), and references therein.
14. G. Rindorf, H. Soling and N. Thorup, *Acta Cryst.*, **C40**, 1137 (1984).
15. P. C. W. Leung, A. J. Schultz, H. H. Wang, T. J. Emge, G. A. Ball, D. D. Cox and J. M. Williams, *Phys. Rev. B: Condens. Matter*, **30**, 1615 (1984).
16. T. J. Emge, J. M. Williams, P. C. W. Leung, A. J. Schultz, M. A. Beno and H. H. Wang, *Mol. Cryst. Liq. Cryst.*, **119**, 237 (1985).
17. S. Kagoshima, T. Yasunaga, T. Ishiguro, H. Anzai and G. Saito, *Solid State Commun.*, **46**, 867 (1983).
18. H. Schwenk, K. Andres and F. Wudl, *Phys. Rev. B: Condens. Matter*, **29**, 500 (1984).
19. (a) J. M. Williams, M. A. Beno, J. C. Sullivan, L. M. Banovetz, J. M. Braam, G. S. Blackman, C. D. Carlson, D. L. Greer, D. M. Loesing and K. Carneiro, *Phys. Rev. B: Condens. Matter*, **B28**, 2873 (1983); (b) J. M. Williams, M. A. Beno, J. C. Sullivan, L. M. Banovetz, J. M. Braam, G. S. Blackman, C. D. Carlson, D. L. Greer and D. M. Loesing, *J. Am. Chem. Soc.*, **105**, 643 (1983).
20. A. Bondi, *J. Phys. Chem.*, **68**, 441 (1964).
21. T. J. Kistenmacher, *Solid State Commun.*, **51**, 275 (1984).
22. H. Kobayashi, R. Kato, T. Mori, A. Kobasyashi, Y. Sasaki, G. Saito, T. Enoki and H. Inokuchi, *Mol. Cryst. Liq. Cryst.*, **107**, 33 (1984).
23. G. Saito, T. Enoki, K. Toriumi and H. Inokuchi, *Solid State Commun.*, **42**, 557 (1982).
24. J. M. Williams, M. A. Beno, H. H. Wang, P. E. Reed, L. J. Azevedo and J. E. Schirber, *Inorg. Chem.*, **23**, 1790 (1984).
25. S. S. P. Parkin, E. M. Engler, R. R. Schumaker, R. Lagier, V. Y. Lee, J. Voiron, K. Carneiro, J. C. Scott and R. L. Greene, *Phys. Rev. Lett.*, **50**, 270 (1983).
26. E. B. Yagubskii, I. F. Shchegolev, V. N. Laukhin, P. A. Kononovich, M. V. Kartsovnik, A. V. Zvarykina and L. I. Buravov, *Pis'ma Zh. Eksp. Teor. Fiz.*, **39**, 12 (1984) [*JETP Lett.*, **39**, 12 (1984)].
27. G. W. Crabtree, K. D. Carlson, L. N. Hall, P. T. Copps, H. H. Wang, T. J. Emge, M. A. Beno and J. M. Williams, *Phys. Rev. B: Condens. Matter*, **30**, 2958 (1984).
28. K. D. Carlson, G. W. Crabtree, L. N. Hall, F. Behroozi, P. T. Copps, L. M. Sowa, L. Nunez, M. A. Firestone, H. H. Wang, M. A. Beno, T. J. Emge and J. M. Williams, *Mol. Cryst. Liq. Cryst.*, **125**, 159 (1985).
29. J. M. Williams, H. H. Wang, M. A. Beno, T. J. Emge, L. M. Sowa, P. T. Copps, F. Behroozi, L. N. Hall, K. D. Carlson and G. W. Crabtree, *Inorg. Chem.*, **23**, 3839 (1984).
30. V. F. Kaminskii, T. G. Prokhorova, R. P. Shibaeva and E. B. Yagubskii, *Pis'ma Zh. Eksp. Theor. Fiz.*, **39**, 15 (1984), [JETP Lett., **39**, 17 (1984)].
31. J. M. Williams, T. J. Emge, H. H. Wang, M. A. Beno, P. T. Copps, L. N. Hall, K. D. Carlson and G. W. Crabtree, *Inorg. Chem.*, **23**, 2558 (1984).
32. K. Bender, I. Hennig, D. Schweitzer, K. Dietz, H. Endres and H. J. Keller, *Mol. Cryst. Liq. Cryst.*, **108**, 359 (1984).
33. T. Mori, A. Kobayashi, Y. Sasaki, H. Kobayashi, G. Saito and H. Inokuchi, *Bull. Chem. Soc. Japan*, **57**, 627 (1984).
34. P. C. W. Leung, M. A. Beno, T. J. Emge, H. H. Wang, M. K. Bowman, M. A. Firestone, L. M. Sowa and J. M. Williams, *Mol. Cryst. Liq. Cryst.*, **125**, 113 (1985).

35. R. Taylor and O. Kennard, *Acta Cryst.*, **B39**, 133 (1983).
36. G. B. Carpenter, *Acta Cryst.*, **20**, 330 (1966).
37. A. F. Wells, "Structural Inorganic Chemistry," Fifth Ed., Oxford University Press, New York, New York, p. 396 (1984).
38. T. J. Emge, P. C. W. Leung, M. A. Beno, A. J. Schultz, H. H. Wang, L. M. Sowa and J. M. Williams, *Phys. Rev. B: Condens. Matter*, **30**, 6780 (1984). Preliminary results from neutron diffraction data of β-(ET)$_2$I$_3$ indicate that the modulated structure at 20 K closely resembles that observed at 120 K (see reference 41).
39. F. J. Dyson, *Phys. Rev.*, **98**, 349 (1955); G. Feher and A. F. Kip, *Phys. Rev.*, **98**, 337 (1955).
40. A. C. Chapman, P. Rhodes and E. F. W. Seymour, *Proc. Phil. Soc.*, B**70**, 345 (1957).
41. (a) P. C. W. Leung, T. J. Emge, M. A. Beno, H. H. Wang, J. M. Williams, V. Petricek and P. Coppens, *J. Am. Chem. Soc.*, **106**, 7644 (1984); (b) P. C. W. Leung, T. J. Emge, M. A. Beno, H. H. Wang and J. M. Williams, *J. Am. Chem. Soc.*, in press (1985).
42. M-H. Whangbo, J. M. Williams, P. C. W. Leung, M. A. Beno, T. J. Emge, H. H. Wang, K. D. Carlson and G. W. Crabtree, *J. Am. Chem. Soc.*, in press (1985).
43. T. J. Emge, H. H. Wang, M. A. Beno, P. C. W. Leung, M. A. Firestone, H. C. Jenkins, J. D. Cook, K. D. Carlson, J. M. Williams, E. L. Venturini, L. J. Azevedo, and J. E. Schirber, *Inorg. Chem.*, **24**, 1736 (1985).
44a. Laboratory student participant sponsored by the Argonne Division of Educational Programs from Indiana University of Pennsylvania.
44b. Undergraduate student participant, sponsored by the Argonne Division of Educational Programs from St. Michaels College, Winooski, VT.